JOURNAL OF GUIDANCE, CONTROL, AND DYNAMICS
Vol. 32, No. 2, March–April 2009

Spin–Yaw Lock-In of a Rotationally Symmetric Missile

Charles H. Murphy*
Upper Falls, Maryland 21156
and
William H. Mermagen
Havre de Grace, Maryland 21087

DOI: 10.2514/1.40052

Spin–yaw lock-in has usually been associated with small aerodynamic asymmetries that produce a trim angle that rotates with the missile. Recent trajectory calculations using wind-tunnel measurements of the aerodynamic moment acting on a rotationally symmetric missile predicted spin–yaw lock-in. Thus, an asymmetry-induced trim moment is not necessary for lock-in. For a side moment that varies with the roll angle between the angle-of-attack plane and a fixed plane on the missile, this paper shows that lock-in of the coning motion and the rolling motion can occur. The conditions on the aerodynamic moments for occurrence of lock-in are derived and appropriate stability criteria are obtained. A simple case of a hypersonic finned missile is considered and the existence of lock-in is demonstrated.

Nomenclature

A	=	$\rho Sd/2$ m
$C_{\ell p}, C_{\ell n}, C_{\ell 0}$	=	roll moment coefficients
$C_{Mq}, C_{M\alpha}, C_{M\dot{\alpha}}, C_{SM}$	=	pitch moment coefficients
$C_{N\alpha}$	=	normal force coefficient
c_0	=	linear static moment coefficient
d	=	missile body diameter
F_x, F_y, F_z	=	aerodynamic force components
H, M, M_{SM}	=	coefficients in Eq. (14)
K_p, K_n	=	coefficients in Eq. (13)
k_t, k_x	=	transverse and axial radii of gyration
I_t, I_x	=	transverse and axial moments of inertia
M_x, M_y, M_z	=	aerodynamic moment components
M_0	=	$Ak_t^{-2}c_0$
m	=	missile mass
p, q, r	=	components of angular velocity
$\hat{p}$	=	pd/V
p_{SS}	=	steady-state roll rate
S	=	reference area
u, v, w	=	missile velocity components
V	=	magnitude of missile velocity
α	=	angle of attack
β	=	angle of sideslip
γ	=	$u/V \cong 1$
δ	=	magnitude of ξ
θ, ψ, ϕ	=	Euler angles of pitch, yaw, and roll
θ	=	orientation angle of ξ
ξ	=	$(v + iw)/V \cong \beta + i\alpha$
ρ	=	air density
σ	=	I_x/I_t
$\propto$	=	$(q + ir)d/V$

Introduction

IF A missile can be rotated through an angle $2\pi/k$ ($k = 3, 4, 5, \ldots$) and it looks the same as the missile in its original orientation, the missile is rotationally symmetric. If the fins of a rotationally symmetric finned missile are slightly canted or slightly deformed, the missile is now asymmetric and its transverse aerodynamic force/moment expressions are augmented by constant-amplitude force/moment terms that rotate with the missile. For constant spin, these terms produce a constant-amplitude trim angle rotating with the missile. The amplitude of this angle is a function of the spin and has a resonance maximum when the spin rate is near the missile's pitch frequency.

Missile designers can control the spin by differentially canting the fins. When this is done, the missile still has rotational symmetry but no longer has mirror symmetry. The spin can be forced to be significantly smaller or larger than the pitch frequency. Unfortunately, nonlinear roll-angle-dependent roll moments exist that can make the spin lock in to the pitch frequency. An important example of such a roll moment is caused by a lateral shift of the missile's center of mass. This roll moment and its effect have been studied by a number of authors [1–5].

Many wind-tunnel measurements of the aerodynamic moment of various symmetric finned missiles have shown a dependence on the roll angle between a fin and the angle-of-attack plane [6–8]. The transverse aerodynamic moment can be expressed in terms of a pitch moment that causes a rotation in the angle-of-attack plane and a side moment that causes rotation perpendicular to the angle-of-attack plane. The linear value of this side moment is zero, but a nonlinear side moment can vary with this roll angle and have nonzero values.

Pepitone and Jacobson [9] have shown that roll-angle-dependent pitch and side moments can have significant effects on the angular motion of a symmetric missile when the spin rate is equal to the coning frequency. Thus, a completely symmetric missile can have a resonance response. This resonance is, however, important only if spin–yaw lock-in can occur for a rotationally symmetric missile.

In a recent paper, Beyer and Costello [10] studied the flight dynamics of flap-controlled open boxes. They made a number of subsonic wind-tunnel measurements of the aerodynamic force and moment acting on various open boxes. These measurements showed the variation of the aerodynamic force and moment with the magnitude of angle of attack and the roll angle of the angle-of-attack plane. These wind-tunnel results were used in six-degree-of-freedom trajectory calculations. For certain center-of-mass locations, lock-in motion occurred. This paper is a study of the theoretical characteristics of this lock-in motion.

Equations of Motion

A missile-fixed coordinate system can be specified with its X axis along the symmetry axis, its Y axis in the plane of a fin, and the Z axis determined by the right-hand rule. The Euler angles θ, ψ, and ϕ relate the missile-fixed system to an Earth-fixed system for which the X

Presented as Paper 6491 at the AIAA Atmospheric Flight Mechanics Conference, Hilton Head, SC, 20–23 August 2007; received 26 July 2008; revision received 27 September 2008; accepted for publication 5 October 2008.

*Consultant. Fellow AIAA.

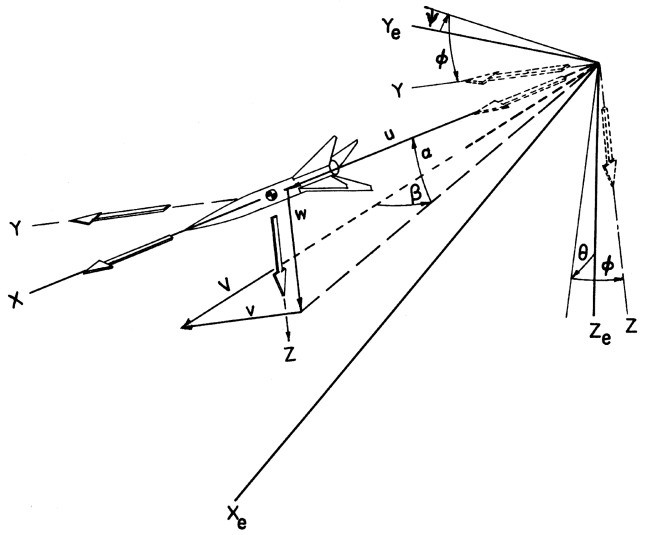

Fig. 1 Missile-fixed and Earth-fixed coordinates.

axis is aligned in the direction of the initial velocity vector (see Fig. 1.)

The velocity vector of the missile's center of mass and the missile angular velocity vector can be described by components along these missile-fixed axes:

$$\mathbf{V} = (u, v, w) \tag{1}$$

$$\mathbf{\Omega} = (p, q, r) \tag{2}$$

The missile is assumed to have a symmetric mass distribution. The coordinates axes are normal axes of inertia, and the moments of inertia along the Y and Z axes are equal Thus, the angular momentum vector is

$$\mathbf{H} = (I_x p, I_t q, I_t r) \tag{3}$$

In view of the missile rotation symmetry, the analysis can be simplified by describing the motion in the Y–Z plane in terms of a complex angle of attack. The complex angle of attack is the angle between the velocity vector and X axis; δ is its magnitude and $\tilde{\theta}$ specifies the orientation of the plane of this angle with respect to the X–Y plane:

$$\xi = \frac{v + iw}{V} = \delta e^{i\tilde{\theta}} = \sin\beta + i\cos\beta\sin\alpha \cong \beta + i\alpha \tag{4}$$

In the usual airplane flight dynamics, α is the angle of attack and β is the sideslip angle.

A complex transverse angular velocity can be defined:

$$\propto = \frac{(q + ir)d}{V} \tag{5}$$

The usual linear expression for the aerodynamic force and moment can be stated in terms of these two complex variables:

$$F_x = (\rho V^2 S/2)C_X \cong -(\rho V^2 S/2)C_D \tag{6}$$

$$F_y + iF_z = -(\rho V^2 S/2)C_{N\alpha}\xi \tag{7}$$

$$M_x = (\rho V^2 Sd/2)[C_{\ell p}(pd/V) + C_{\ell 0}] \tag{8}$$

$$M_y + iM_z = (\rho V^2 Sd/2) \times [(C_{SM} - iC_{M\alpha})\xi - iC_{M\dot{\alpha}}(\dot{\xi} + ip\xi)(d/V) + C_{Mq} \propto] \tag{9}$$

The constant roll moment in the second term in Eq. (8) is usually created by differentially canting the fins. This causes the missile to fly at a constant-steady-state spin:

$$p_{ss}d/V = -C_{\ell 0}/C_{\ell p} \tag{10}$$

Linear flight dynamics show that the pitch moment coefficient $C_{M\alpha}$ controls the frequencies of the motion, and the damping coefficients $C_{M\dot{\alpha}}$ and C_{Mq} control the growth or decay of the motion.

In this paper we will assume that C_{SM} and $C_{M\alpha}$ are functions of δ and $\tilde{\theta}$, and we will add a nonlinear induced-roll-moment term to the axial moment:

$$M_x = (\rho V^2 Sd/2)[C_{\ell p}(p - p_{ss})(d/V) + \delta C_{\ell n}(\delta, \tilde{\theta})] \tag{11}$$

The missile's rotational symmetry requires these three nonlinear aerodynamic coefficients to be periodic functions of $\tilde{\theta}$ with a period of $2\pi/k$. Points on the surface of the missile can be located by three coordinates: x, y, and z. If they are relocated to x, y, and $-z$ and the result looks the same, the missile has mirror symmetry. If the missile has mirror symmetry, C_{SM} and $C_{\ell\delta}$ are odd functions of $\tilde{\theta}$, and $C_{M\alpha}$ is an even function of $\tilde{\theta}$.

The differential equations of motion can be obtained by differentiating the linear and angular momentum and equating them to the aerodynamic force and moment. The independent variable t is replaced by nondimensional arc length s:

$$s = d^{-1}\int_0^t V\mathrm{d}t \tag{12}$$

The resulting vector equations for the angular motion can be written as six first-order real equations.

The drag and roll equations are

$$V'/V = -AC_D \tag{13}$$

$$\hat{p}' + K_p(\hat{p} - \hat{p}_{ss}) + K_n(\delta, \tilde{\theta}) = 0 \tag{14}$$

where

$$K_p = -A(k_x^{-2}C_{\ell p} - C_D) \qquad K_n = -Ak_x^{-2}\delta C_{\ell n}(\delta, \tilde{\theta})$$

$$k_x = \sqrt{\frac{I_x}{md^2}} \qquad A = \frac{\rho Sd}{2\text{ m}} \qquad \hat{p} = \frac{pd}{V}$$

and primes denote derivatives with respect to s.

The y and z components of the equations for the derivatives of the linear and angular momentum are

$$\dot{v} - pw + ru = AC_y(V^2/d) \tag{15}$$

$$\dot{w} + pv - qu = AC_z(V^2/d) \tag{16}$$

$$\dot{q} - (1 - \sigma)r = Ak_t^{-2}C_m(V/d)^2 \tag{17}$$

$$\dot{r} + (1 - \sigma)q = Ak_t^{-2}C_n(V/d)^2 \tag{18}$$

where

$$\sigma = I_x/I_y \qquad k_t = \sqrt{I_t/md^2}$$

Equations (16) and (18) are multiplied by i and added to Eqs. (15) and (17), respectively, the independent variable is changed from t to s, and the complex variables ξ and $\propto$ are introduced:

$$\xi' - (AC_D - i\hat{p})\xi - i\gamma \propto = A(C_y + iC_z) \tag{19}$$

$$\propto' -[AC_D - i\hat{p}(1-\sigma)] \propto = Ak_t^{-2}(C_m + iC_n) \tag{20}$$

where

$$\gamma = u/V = (1-\delta^2)^{1/2} \cong 1$$

Finally, $\propto$ is eliminated between the two differential equations to yield a second-order complex equation describing the angular motion [11]. Finally, the force and moment expressions of Eqs. (7) and (9) are inserted. (Because A is quite small, squares of A have been neglected.)

$$\xi'' + [H - i(\sigma-2)\hat{p}]\xi' + [(\sigma-1)(\hat{p})^2 - M + i(\hat{p}' + \hat{p}H - M_{SM})]\xi = 0 \tag{21}$$

where

$$H = A[C_{N\alpha} - 2C_D - k_t^{-2}(C_{Mq} + C_{M\dot{\alpha}})]$$
$$M = Ak_t^{-2}C_{M\alpha}(\delta, \tilde{\theta}) \qquad M_{SM} = Ak_t^{-2}C_{SM}(\delta, \tilde{\theta})$$

Spin–Yaw Lock-In

Lock-in motion can be defined as motion for which the spin is constant and the complex angle of attack is constant in missile-fixed coordinates. Thus,

$$\hat{p}' = \xi'' = \xi' = 0 \tag{22}$$

In nonspinning coordinates, the missile is moving in a constant-amplitude coning motion at the spin rate. The spin rate, amplitude, and phase angle for this equilibrium motion will be denoted as p_e, δ_e, and $\tilde{\theta}_e$. The three conditions for the three lock-in parameters can be obtained from Eqs. (14) and (21) by use of Eq. (22):

$$K_n(\delta_e, \tilde{\theta}_e) = K_p(p_{ss} - p_e)(d/V) \tag{23}$$

$$M_{SM}(\delta_e, \tilde{\theta}_e) = \hat{p}_e H \tag{24}$$

$$p_e(d/V) = \pm\sqrt{-M(\delta_e, \tilde{\theta}_e)/(1-\sigma)} \tag{25}$$

According to Eq. (24), the side moment affects the damping of the motion.

Stability of Equilibrium Motion

Motion near equilibrium can be described by small perturbation functions:

$$\hat{p} = \hat{p}_e + \eta_1(s) \tag{26}$$

$$\delta = \delta_e + \eta_2(s) \tag{27}$$

$$\tilde{\theta} = \tilde{\theta}_e + \eta_3(s) \tag{28}$$

These perturbation functions are assumed to be exponential functions of s:

$$\eta_j = \eta_{j0}e^{\lambda s} \quad (j = 1, 2, 3) \tag{29}$$

Equations (26–28) are inserted in Eqs. (14) and (21). Three equations in the three unknowns η_{j0} follow from Eq. (14) and the real and imaginary parts of Eq. (21):

$$\sum_{j=1}^{3} a_{ij}\eta_{j0} = 0 \quad (i = 1, 2, 3) \tag{30}$$

Expressions for the coefficients in Eq. (30) are given next:

$$a_{11} = \lambda + K_p \qquad a_{12} = K_{n5} \qquad a_{13} = K_{n\theta} \qquad a_{21} = \delta_e(\lambda + H)$$
$$a_{22} = (2-\sigma)\hat{p}_e\lambda - \delta_e M_{SM\delta} \qquad a_{23} = \delta_e(\lambda^2 + H\lambda - M_{SM\theta})$$
$$a_{31} = -2\delta_e(1-\sigma)\hat{p}_e \qquad a_{32} = \lambda^2 + H\lambda - \delta_e M_\delta$$
$$a_{33} = -\delta_e[(2-\sigma)\hat{p}_e\lambda + M_\theta]$$

where

$$K_{n\theta} = \frac{\partial K_n}{\partial\tilde{\theta}} \qquad K_{n\delta} = \frac{\partial K_n}{\partial\delta} \qquad M_{SM\theta} = \frac{\partial M_{SM}}{\partial\tilde{\theta}}$$
$$M_{SM\delta} = \frac{\partial M_{SM}}{\partial\delta} \qquad M_\theta = \frac{\partial M}{\partial\tilde{\theta}} \qquad M_\delta = \frac{\partial M}{\partial\delta}$$

Equation (30) will have a solution when the determinant of the coefficients is zero. This yields a fifth-order polynomial:

$$\lambda^5 + d_4\lambda^4 + d_3\lambda^3 + d_2\lambda^2 + d_1\lambda + d_0 = 0 \tag{31}$$

The five coefficients in Eq. (31) are as follows:

$$d_4 = 2H + K_p$$

$$d_3 = 2HK_p - \delta_e M_\delta - M_{SM\theta} + H^2 - K_{n\theta} + (2-\sigma)^2(\hat{p}_e)^2$$

$$d_2 = K_p[H^2 + (2-\sigma)^2(\hat{p}_e)^2] - (H + K_p)(\delta_e M_\delta + M_{SM\theta}) + (2-\sigma)\hat{p}_e(M_\theta - \delta_e M_{SM\delta}) - \sigma\delta_e\hat{p}_e K_{n\delta} - 2HK_{n\theta}$$

$$d_1 = M_{SM\theta}\delta_e M_\delta - M_\theta\delta_e M_{SM\delta} - HK_p(\delta_e M_\delta + M_{SM\theta}) - \delta_e K_{n\delta}(M_\theta + \sigma\delta_e\hat{p}_e) + b$$

$$d_0 = (K_p M_{SM\theta} + HK_{n\theta})\delta_e M_\delta - \delta_e HK_{n\delta}M_\theta + [2(1-\sigma)\hat{p}_e K_{n\theta} - K_p M_\theta]\delta_e M_{SM\delta} - 2(1-\sigma)\hat{p}_e\delta_e K_{n\delta}M_{SM\theta}$$

where

$$b = -[2(2-\sigma)(1-\sigma)(\hat{p}_e)^2 + H^2 - \delta_e M_\delta]K_{n\theta} + (2-\sigma)\hat{p}_e K_p(M_\theta - \delta_e M_{SM\delta})$$

Equation (31) specifies five possible values of λ. For a stable equilibrium state, the real parts of these roots of Eq. (24) must be negative. These roots are numerically calculated to determine stability.

Simple Example

Very simple nonlinear functions will now be specified:

$$C_{\ell n} = -a_1(C_{\ell p} - k_x^2 C_D)\delta\sin k\tilde{\theta} \tag{32}$$

$$C_{SM} = a_2 c_0 \sin k\tilde{\theta} \tag{33}$$

$$C_{M\alpha} = c_0(1 - c_1\delta^2 + a_3\cos k\tilde{\theta}) \tag{34}$$

For the simple functions defined by Eqs. (32–34), Eqs. (23–25) reduce to

$$a_1\delta_e\sin k\tilde{\theta}_e = (p_e - p_{ss})d/V \tag{35}$$

$$a_2\sin k\tilde{\theta}_e = \frac{H}{M_0}\frac{p_e d}{V} \tag{36}$$

$$p_e d/V = \pm\sqrt{-M_0(1 - c_1\delta_e^2 + a_3\cos k\tilde{\theta}_e)/(1-\sigma)} \qquad (37)$$

where $M_0 = Ak_t^{-2}c_0$.

The partial derivatives of the Eq. (30) coefficients can be computed using the functions defined by Eqs. (32–34), and they are given as follows:

$$K_{n\theta} = kAa_1(k_x^{-2}C_{\ell p} - C_D)\delta_e \cos k\tilde{\theta}_e$$

$$K_{n\delta} = Aa_1(k_x^{-2}C_{\ell p} - C_D)\sin k\tilde{\theta}_e$$

$$M_{SM\theta} = kM_0 a_2 \cos k\tilde{\theta}_e$$

$$M_{SM\delta} = 0$$

$$M_\theta = -kM_0 a_3 \sin k\tilde{\theta}_e$$

$$M_\delta = -2M_0 c_1 \delta_e$$

We will consider the long hypersonic missile with four symmetric fins and a fineness ratio of 20 that was used in [5]. Its physical and aerodynamic characteristics are given next:

$$k = 4 \qquad p_{ss} = 0 \qquad d = 0.35 \text{ ft} \qquad S = \pi d^2/4$$
$$V = 6000 \text{ ft} \qquad m = 3.5 \text{ slug} \qquad I_x = 0.054 \text{ slug}\cdot\text{ft}^2$$
$$I_t = 14.3 \text{ slug}\cdot\text{ft}^2 \qquad \rho = 0.002 \text{ slug/ft}^3 \qquad C_{lp} = -18$$
$$c_0 = 6.0 \qquad c_1 = \delta_T^{-2} = 25 \qquad C_D = 0.4 \qquad C_{L\alpha} = 6.0$$
$$a_1 = 0.0069 \qquad a_2 = 0.4747 \qquad a_3 = 0$$
$$C_{Mq} + C_{M\dot{\alpha}} = -1180$$

For the preceding parameters, Eqs. (35–37) yield values for p_e and δ_e. They are ± 4.02 rps and 0.30 (17 deg) There are two families of $\tilde{\theta}_e$ for positive spin and another two families for negative spin. For $\tilde{\theta}_e$ in degrees, they are

$$p_e > 0 \qquad \tilde{\theta}_e = 11.25 + 90j \qquad 33.75 + 90j \qquad (j = 0, 1, 2, 3) \qquad (38)$$

$$p_e < 0 \qquad \tilde{\theta}_e = -11.25 + 90j \qquad -33.25 + 90j \qquad (j = 0, 1, 2, 3) \qquad (39)$$

The roots of polynomial (31) are computed for the four families. According to the real parts of these roots, both first families in Eqs. (38) and (39) are stable and both second families are unstable.

The actual occurrence of spin–yaw lock-in is demonstrated by two numerical integrations of Eqs. (14) and (21). For all calculations, $\tilde{\theta}_0 = 33$ deg and $\xi_0' = 0$, and the initial conditions for δ and p will be specified as multiples of the equilibrium conditions:

$$\delta_0 = R_\delta \delta_e \qquad p_0 = R_p|p_e| \qquad (40)$$

For the first case, $R_\delta = 1$ and $R_p = 0.7$, and for the second case, $R_\delta = 1$ and $R_p = 0.5$.

Figures 2–5 give the results for the first case. Figure 2 shows p approaching its equilibrium value of 4.02 rps after some large oscillations. In Fig. 3, δ approaches its equilibrium value of 0.3, and in Fig. 4, $\tilde{\theta}$ approaches its equilibrium value of 191. This corresponds to the third member of the stable family for positive spin. Finally,

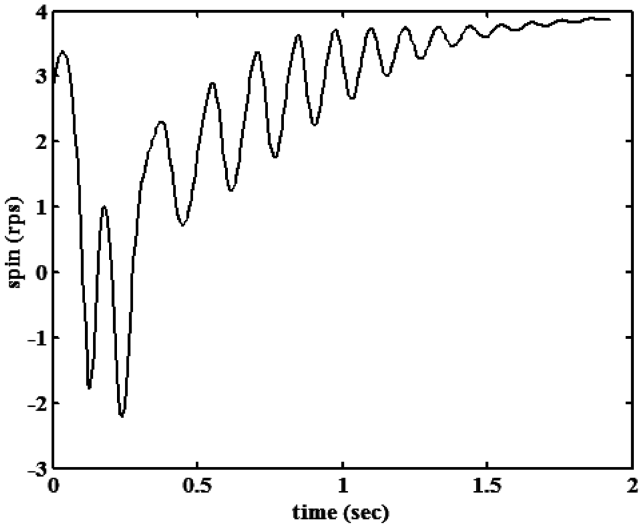

Fig. 2 Spin versus time; $R_\delta = 1$ and $R_b = 0.7$.

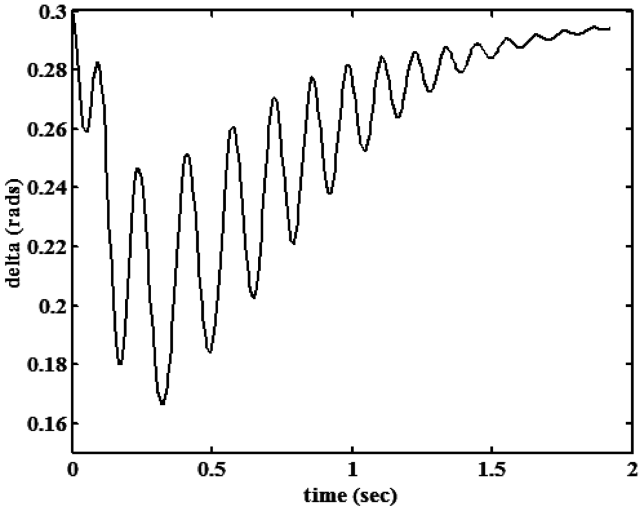

Fig. 3 Delta versus time; $R_\delta = 1$ and $R_b = 0.7$.

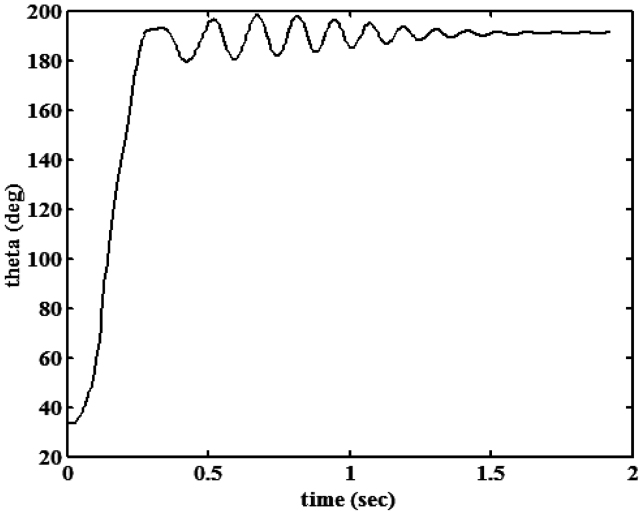

Fig. 4 Theta versus time; $R_\delta = 1$ and $R_b = 0.7$.

Fig. 5 plots α versus β and shows that the angular motion starts in the first quadrant and ends in the third quadrant.

For second case, Fig. 6 shows a decrease of p to an equilibrium value of -4.02 rps. Figure 7 shows that δ approaches its equilibrium

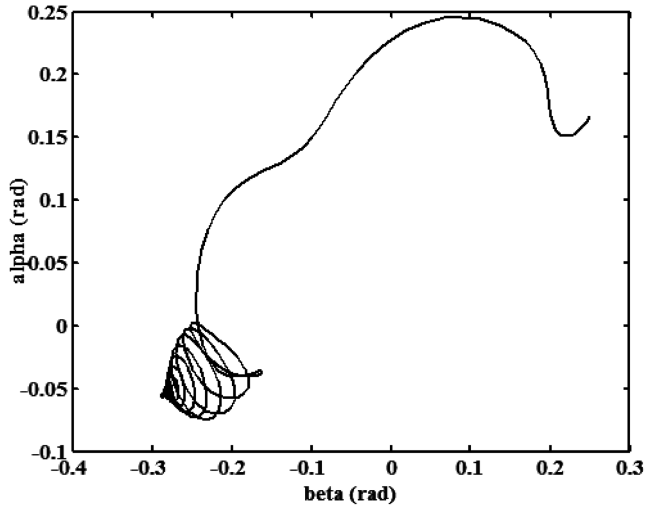

Fig. 5 Alpha versus beta; $R_\delta = 1$ and $R_b = 0.7$.

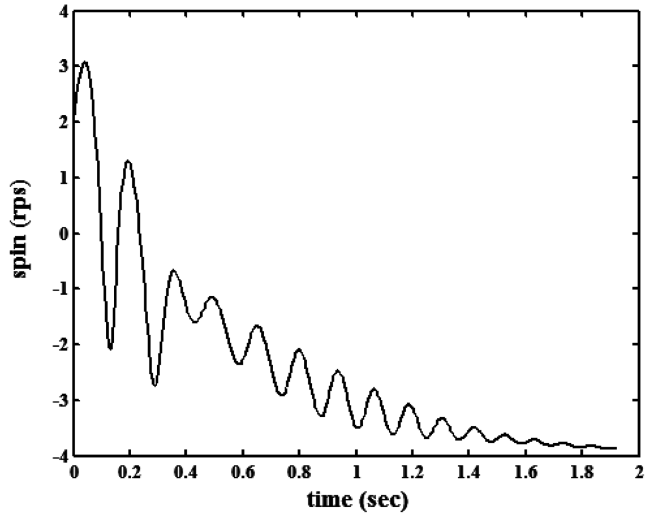

Fig. 6 Spin versus time; $R_\delta = 1$ and $R_b = 0.5$.

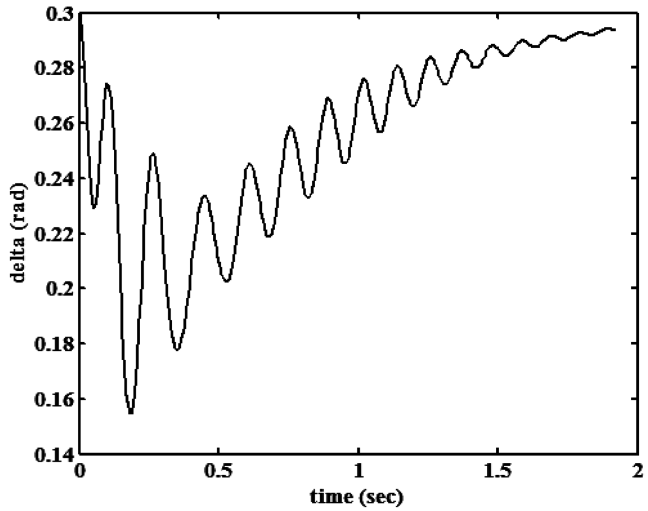

Fig. 7 Delta versus time; $R_\delta = 1$ and $R_b = 0.5$.

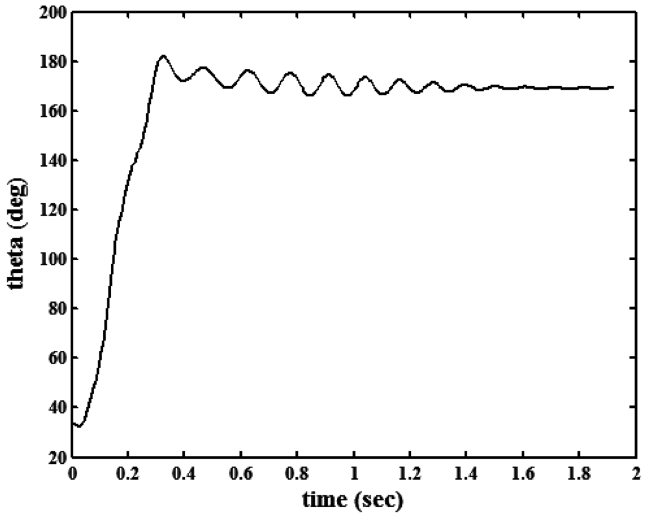

Fig. 8 Theta versus time; $R_\delta = 1$ and $R_b = 0.5$.

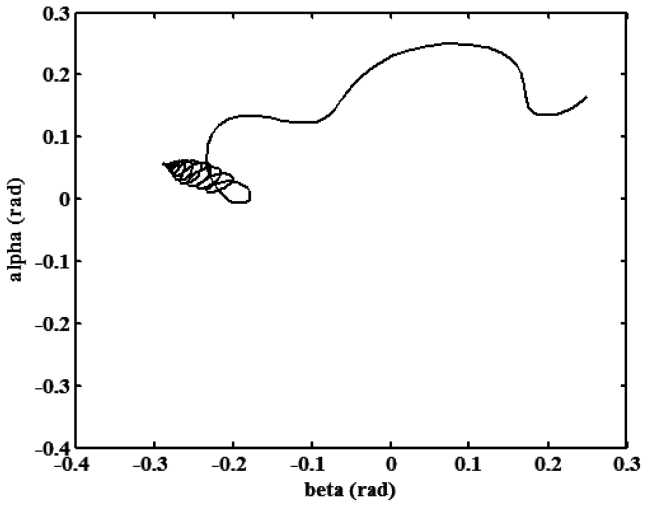

Fig. 9 Alpha versus beta; $R_\delta = 1$ and $R_b = 0.5$.

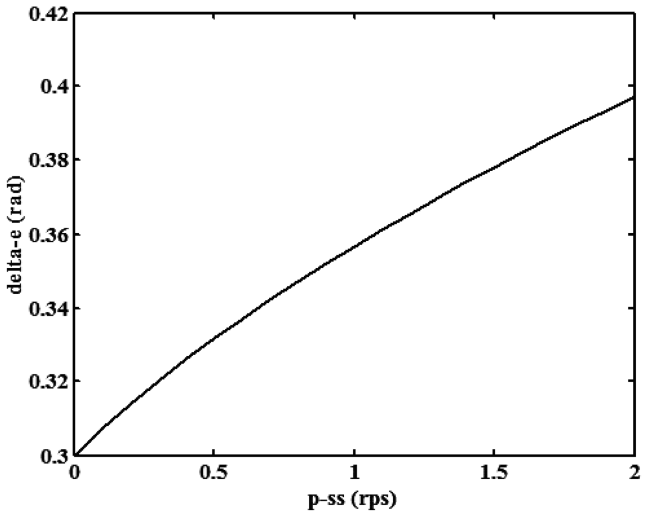

Fig. 10 Delta-*e* versus steady-state spin.

value of 0.3, and in Fig. 8, $\tilde{\theta}$ approaches its equilibrium value of 169. This corresponds to the third member of the stable family for negative spin. Figure 9 plots α versus β and shows the motion starting in the first quadrant and ending in the second quadrant. A number of integrations were made for other values of R_δ and R_p, and for all cases, either positive lock-in or negative lock-in occurred.

If the steady-state spin is not zero, different equilibrium values are obtained. Figure 10 plots equilibrium amplitude versus steady-state

spin. We see that increasing steady-state spin increases δ. According to Eq. (37), this increases the magnitude of lock-in spin. The occurrence of positive or negative spin is a function of initial conditions.

Conclusions

We have shown that lock-in can occur for rotational symmetric missiles. This lock-in can also occur when the fins are differentially canted to produce a design steady-state spin. The occurrence of positive or negative lock-in spin is determined by initial conditions.

References

[1] Grover, L. S., "Effects on Roll Rate of Mass and Aerodynamic Asymmetries of Ballistic Re-Entry Bodies," *Journal of Spacecraft and Rockets*, Vol. 2, No. 2, Mar.–Apr. 1965, pp. 220–225. doi:10.2514/3.28154

[2] Price, D. A., Jr., "Sources, Mechanisms, and Control of Roll Resonance Phenomena for Sounding Rockets," *Journal of Spacecraft and Rockets*, Vol. 4, No. 11, Nov. 1967, pp. 1516–1523. doi:10.2514/3.29122

[3] Price, D. A., Jr., and Ericsson, L. E., "A New Treatment of Roll-Pitch Coupling for Ballistic Re-Entry Vehicles," *AIAA Journal*, Vol. 8, No. 9, Sept. 1970, pp. 1608–1615. doi:10.2514/3.5954

[4] Murphy, C. H., "Some Special Cases of Spin-Yaw Lockin," *Journal of Guidance and Control*, Vol. 12, No. 6, Nov.–Dec. 1989, pp. 771–776. doi:10.2514/3.20480

[5] Murphy, C. H., and Mermagen, W. H., "Spin-Yaw Lockin of an Elastic Finned Missile," *Journal of Guidance, Control, and Dynamics*, Vol. 28, No. 1, Jan.–Feb. 2005, pp. 121–130. doi:10.2514/1.4573

[6] Reece, E. W., "Six Component Force Test of the TX-61 at Mach 0.7 to 2.5 with Varying Angles of Attack and Roll Angles," Sandia Labs., Rept. SC-JM-65-575, Albuquerque, NM, Feb. 1966.

[7] Reece, E. W., "Results of a Wind Tunnel Test to Determine the Effect of Roll Position on the Longitudinal Static Stability of the Tomahawk Rocket Configuration at Mach 7.3," Sandia Labs., Rept. SC-TM-495, Albuquerque, NM, Oct. 1966.

[8] Regan, F. J., Shermerhorn, V. W., and Falusi, M. E., "Roll-Induced Force and Moment Measurements of the M823 Research Store," U. S. Naval Ordinance Lab., Rept. NOLTR 68-195, White Oak, MD, Nov. 1968.

[9] Pepitone, T. R., and Jacobson, I. D., "Resonant Behavior of a Symmetric Missile Having Roll Orientation-Dependent Aerodynamics," *Journal of Guidance and Control*, Vol. 1, No. 5, Sept.–October 1978, pp. 335–339. doi:10.2514/3.55789

[10] Beyer, E., and Costello, M., "Flight Dynamics and Control Authority of Flap-Controlled Open Boxes," *Journal of Guidance, Control, and Dynamics*, Vol. 30, No. 3, May–June 2007, pp. 827–834. doi:10.2514/1.25301

[11] Murphy, C. H., "Free Flight Motion of Symmetric Missiles," Ballistic Research Lab., Rept. 1216, Aberdeen Proving Ground, MD, July 1963.